



HAL
open science

The high resolution Fourier-transform chemiluminescence spectrum of the HS2 radical

Stephen Hugh Ashworth, Ewald H Fink

► **To cite this version:**

Stephen Hugh Ashworth, Ewald H Fink. The high resolution Fourier-transform chemiluminescence spectrum of the HS2 radical. *Molecular Physics*, 2007, 105 (05-07), pp.715-725. 10.1080/00268970601146880 . hal-00513069

HAL Id: hal-00513069

<https://hal.science/hal-00513069>

Submitted on 1 Sep 2010

HAL is a multi-disciplinary open access archive for the deposit and dissemination of scientific research documents, whether they are published or not. The documents may come from teaching and research institutions in France or abroad, or from public or private research centers.

L'archive ouverte pluridisciplinaire **HAL**, est destinée au dépôt et à la diffusion de documents scientifiques de niveau recherche, publiés ou non, émanant des établissements d'enseignement et de recherche français ou étrangers, des laboratoires publics ou privés.



The high resolution Fourier-transform chemiluminescence spectrum of the HS₂ radical

Journal:	<i>Molecular Physics</i>
Manuscript ID:	TMPH-2006-0063.R1
Manuscript Type:	Full Paper
Date Submitted by the Author:	27-Nov-2006
Complete List of Authors:	Ashworth, Stephen; University of East Anglia, School of Chemical Sciences and Pharmacy Fink, Ewald; Bergische Universität Wuppertal, Physikalische Chemie-Fachbereich C
Keywords:	Thiosulfeno radical, chemiluminescence, Fourier-transform spectroscopy, rotational analysis



1
2
3
4
5
6
7
8
9
10
11
12
13
14
15
16
17
18
19
20
21
22
23
24
25
26
27
28
29
30
31
32
33
34
35
36
37
38
39
40
41
42
43
44
45
46
47
48
49
50
51
52
53
54
55
56
57
58
59
60

Equation Section 1

Catchline (head of first page only) *Molecular Physics*, Vol. X, No. X, Month 200x, xxx–xxx

Running heads (verso) *S. H. Ashworth and E. H. Fink*
(recto) *FT chemiluminescence spectrum of HS₂*

Article Type (e.g. Review Article, Research Note, Brief Communication – if known)

For Peer Review Only

The high resolution Fourier-transform chemiluminescence spectrum of the HS₂ radical

Stephen H. Ashworth*† and Ewald H. Fink‡

† The School of Chemical Sciences and Pharmacy, University of East Anglia, Norwich, NR4
7TJ, UK.

‡ Physikalische Chemie-Fachbereich C, Bergische Universität Wuppertal, D-42097
Wuppertal, Germany

*Corresponding author. Email: S.Ashworth@uea.ac.uk

Abstract

The chemiluminescence spectrum of the HS₂ radical has been recorded with a Fourier-transform spectrometer. The overview spectrum in the region 9000 cm⁻¹ to 4000 cm⁻¹ has been analysed and the vibrational parameters obtained are presented. In addition three of the bands (0₀⁰, 3₀¹ and 3₁⁰) which have been recorded at high resolution have been rotationally analysed and the results of the fit are presented. The results are discussed in the context of previous theoretical and experimental studies.

Keywords: Thiosulfeno radical; rotational analysis; chemiluminescence; Fourier-transform spectroscopy;

Introduction

The HS₂ radical was first detected in 1950 during early flash-photolysis studies of hydrogen sulphide [1]. The new band systems were red-degraded, transient and diffuse between 315 and 380 nm. Porter's assignment was supported by later work where these new band systems were shown to occur much more strongly in the flash-photolysis of hydrogen disulphide [2].

A detailed theoretical study by Gosavi et al. [3] used a semi-empirical open-shell CNDO calculation to suggest these bands were the lowest-energy ${}^2A' \leftarrow {}^2A''$ electronic transition of HS₂. This interpretation was questioned by Sannigrahi et al. [4] who pointed out that the analogous transitions of the isovalent HO₂ and HSO radicals had been found at much lower energies experimentally as well as in *ab initio* SCF and CI calculations. These authors carried out detailed calculations of the energies, molecular structure, potential curves, and vibrational constants of HS₂ and DS₂ in their low-lying electronic states and of f-values for various transitions. They assigned the strong UV absorption system to a ${}^2A'' \leftarrow \tilde{X} {}^2A''$ transition and predicted the lowest energy ${}^2A'$ state of HS₂ to lie at 0.85 eV with very similar characteristics as in the isovalent radicals HO₂ and HSO.

Stimulated by these predictions and earlier experimental work on HO₂ [5] and HSO [6], Holstein et al. [7] studied the near-infrared chemiluminescence spectrum of HS₂ excited by energy transfer from metastable singlet oxygen in a fast-flow system. They observed a new band system in the range 1100-1700 nm for both, HS₂ and DS₂, and attributed the bands to the $\tilde{A} {}^2A' \rightarrow \tilde{X} {}^2A''$ transitions of the radicals. Initial work was at low resolution but this still enabled the investigators to make several important observations. Not only were the wavenumbers of the ν_3 vibrations in both electronic states determined but also the ν_2 vibrational wavenumber in the $\tilde{X} {}^2A''$ state was observed. In addition band contour analysis allowed estimates of the rotational constants to be made. It was this analysis which first

1
2 indicated that a significant degree of unexpected $\Delta K_a = 0$ character was present in the band
3
4 contour.

5
6 The ground state of this radical has been well characterised spectroscopically. First,
7
8 Yamamoto and co-workers recorded and analysed the spectrum of both HS₂ and DS₂ in the
9
10 microwave region [8]. Later, HS₂ was discovered by Ashworth et al. during work on the far
11
12 infra-red laser magnetic resonance (LMR) spectrum of the SH radical [9]. Subsequently
13
14 further recordings were made and the FIR LMR spectrum analysed [10]. Further work on the
15
16 ground state has been carried out by Winnewisser and co-workers [11] in the millimetre wave
17
18 region.

19
20 The HS₂ radical continues to be of interest both theoretically and experimentally. On the one
21
22 hand its analogues HO₂ and HSO are important in a variety of environments, notably
23
24 combustion and the oxidation of reduced forms of sulfur [12, 13]. On the other it can be
25
26 regarded as the simplest species with a S-S bond and as such the proton affinity [14] and the
27
28 matrix isolated photolysis products of H₂S₂ [15] have been investigated. In addition there
29
30 have been further attempts to predict the equilibrium structure and other properties of the
31
32 radical *ab initio* [16, 17]. The most recent of these and only the second to calculate
33
34 properties of the excited state is by Denis [18].

35
36 This paper deals with the analysis of both low and high resolution Fourier-transform
37
38 chemiluminescence spectra of the HS₂ radical recorded at the University of Wuppertal. The
39
40 vibrational parameters from the analysis of the low resolution spectra are first presented. The
41
42 results of the analysis of three of the electronic bands ($0_0^0, 3_0^1$ and 3_1^0) are reported and
43
44 compared with the earlier low-resolution results.
45
46

47 Experimental

48
49 The experiments were carried out in a fast-flow system using a 120 cm long Pyrex tube of
50
51 6 cm diameter with quartz windows at both ends as the observation volume. The tube was
52
53
54
55
56
57
58
59
60

Comment [SHA1]: Deleted "hand"

Comment [SHA2]: Citation moved

Comment [SHA3]: Text and citation

Comment [SHA4]: "has" replaced by
"have"

Comment [SHA5]: Numbering
changed

Comment [SHA6]: Numbering
changed

1
2 equipped with two glass inlet systems of smaller diameter and a pumping port. In one inlet
3 system, $\text{HS}_2(\text{DS}_2)$ radicals were generated by reacting $\text{H}(\text{D})$ atoms with sulfur vapor (S_x). A
4 mixture of 5-10 Pa $\text{H}_2(\text{D}_2)$ and 100-150 Pa helium was passed through a 100 W microwave
5 discharge and over molten sulfur contained in a 0.5 L glass vessel which was heated to about
6
7
8
9
10 150° C. In the second inlet system, metastable oxygen molecules, $\text{O}_2(a^1\Delta_g)$, were generated
11
12 by passing 100-150 Pa O_2 with a trace of mercury vapor through a second microwave
13
14 discharge. The film of HgO forming behind the discharge on the wall of the inlet system
15
16 served to remove most of the oxygen atoms from the gas flow. The $\text{O}_2(a^1\Delta_g)$ molecules
17
18 served as energy carriers and were used to excite the $\text{HS}_2(\text{DS}_2)$ radicals in the observation
19
20 tube to their \tilde{A}^2A' state by near-resonant electronic-to-electronic (E-E) energy exchange. The
21
22 system was pumped with a $500 \text{ m}^3\text{h}^{-1}$ roots pump in series with a $30 \text{ m}^3\text{h}^{-1}$ forepump resulting
23
24 in flow velocities of about 20 ms^{-1} in the large diameter tube. The total pressure, as measured
25
26 with a Baratron capacitance manometer, was in the range 200-300 Pa and consisted of about
27
28 equal partial pressures of O_2 and He and < 20 Pa of sulfur containing compounds.
29

30
31 The near-infrared radiation emitted along the axis of the glass tube was focused onto the
32
33 entrance iris of a Bruker IFS 120 HR Fourier-transform spectrometer with a quartz lens. A
34
35 mirror was placed at the far end of the observation tube and aligned so that the signal at the
36
37 entrance aperture was maximised. Spectra were measured in the range $3\,500 - 10\,000 \text{ cm}^{-1}$
38
39 at nominal resolutions of 2 cm^{-1} to 0.01 cm^{-1} using liquid-nitrogen-cooled germanium
40
41 (Applied Detector Corp. Model 403 S) or InSb (Cincinnati Electronics Corp. Model IDH
42
43 100) detectors. The latter was equipped with a cooled $2.8 \mu\text{m}$ short-pass filter. All gases and
44
45 chemicals were research grade and were used without further purification. The wavenumber
46
47 scale of the spectrometer was calibrated by use of reference lines of the $\text{O}_2(a \rightarrow X)$ band [19]
48
49 which showed up in all spectra. The absolute error of the given vacuum wavenumbers is less
50
51
52
53
54
55
56
57
58
59
60

Comment [SHA7]: Replaced "l" with "L"

Comment [SHA8]: Numbering changed. This citation added to list

than $\pm 0.005 \text{ cm}^{-1}$, and the relative precision of wavenumbers of strong lines is on the order of 10^{-4} cm^{-1} .

Results and Analysis

Figure 1 about here

Figures 1a and 1b show overview spectra of the $\tilde{A}^2A' \rightarrow \tilde{X}^2A''$ transitions of HS_2 and DS_2 recorded at low spectral resolution (2 cm^{-1}) in the sensitivity range of the Ge detector. The dominant features in both spectra are some short sequences of $00\nu'_3 - 00\nu''_3$ bands and the 0-0 band of the $b^1\Sigma_g^+ \rightarrow X^3\Sigma_g^-$ transition of S_2 near $8\,000 \text{ cm}^{-1}$. As in the low-resolution work of Holstein *et al.* [7] some weaker features which show up in the spectrum of HS_2 but not in that of DS_2 are tentatively assigned to bands involving transitions in the bending mode. For HS_2 , the spectrum has also been measured in the range $4\,000 - 9\,000 \text{ cm}^{-1}$ with the less sensitive InSb detector. As is seen from Figure 2, two more sequences of the $\Delta\nu_3 = \text{const.}$ series are observed. A weak band at $4\,560 \text{ cm}^{-1}$ which does not belong to this series is tentatively assigned to the $\tilde{A}^2A'(000) \rightarrow \tilde{X}^2A''(100)$ transition.

Figure 2 about here

As is seen from the figures, the $00\nu'_3 - 00\nu''_3$ bands show characteristic sharp peaks at their short wavelength sides. By comparison with high-resolution spectra which have been rotationally analysed (see below) it is seen that the peaks consist mostly of the R lines and low- N Q and P lines of the $\Delta K_a = +1$ sub-bands and possibly of weak but very dense R lines of $\Delta K_a = 0$ sub-bands. Such $\Delta K_a = 0$ bands, which are “forbidden” in perpendicular transitions, have been identified in the analogous bands of HO_2 and were found to be mainly due to magnetic dipole transitions [20, 21]. In band contour analyses of the low-resolution bands, $\Delta K_a = 0$ sub-bands were also needed for HS_2 to fit the calculated and experimental band contours [7]. For the 001-000, 000-000, and 000-001 bands, which have been measured

Comment [SHA9]: Numbering changed

Comment [SHA10]: Citation added



at high resolution and rotationally analysed (see below), the wavenumbers of the peaks are respectively 8.2, 8.5, and 9.0 cm^{-1} larger than those of the corresponding band origins.

Wavenumbers of the sharp peaks have been measured for 18 bands of HS_2 and 7 bands of DS_2 , and were fitted to Equation (1) [22]

$$\nu(v_3' - v_3'') = \nu_0 + \omega_3^0 v_3' + x_{33}^0 v_3'^2 - \omega_3^0 v_3'' - x_{33}^0 v_3''^2, \quad (1)$$

where ν_0 is the energy separation of the $\tilde{A}^2A'(000)$ and $\tilde{X}^2A''(000)$ vibrational ground states and ω_3^0 and x_{33}^0 are parameters the sum of which yields the vibrational quantum ν_3 .

The wavenumbers of the bands and the observed-calculated differences are given in Table 1.

The results of the fit and other data deduced from the low-resolution spectra are collected in Table 2.

Table 1 about here

Table 2 about here

The spectrum of HS_2 in the range 6 400 – 8 100 cm^{-1} was measured at a nominal resolution of 0.01 cm^{-1} and showed apodized line half-widths of 0.016 cm^{-1} . An overview spectrum of the 000-000 and 001-001 bands is shown in Figure 3. Neither individual rotational lines nor coarse K_a structure are obvious in this spectrum. An expanded portion of the 001-000 band

Comment [SHA12]: "000-001" replaced by "001-000"

is shown in Figure 4. The most obvious features in each band are two series of strong doublets, where the splitting of each pair of lines slowly decreases as one moves to lower wavenumbers. The spacing between doublets is, however, steadily increasing. At the start of the analysis these two features were assumed to be the Q-branch lines of the $K_a = 1-0$ and $K_a = 0-1$ subbands respectively.

Figure 3 about here

Figure 4 about here

The ground state of the HS_2 radical has already been well characterised [8, 10, 11] and the energy levels for the ground state can be calculated with confidence. The data in this work have been analysed using a program based on the asymmetric rotor program originally developed by Brown and Sears [23] and released into the public domain as ASYTOP [24].

Comment [SHA13]: Numbering changed. Citation added to list.

Comment [SHA14]: Numbering changed. Citation moved from where [23] now is.

Having calculated the position of the levels with $K_a = 1$ in the lower state, common differences were calculated and each Q-branch line tested for the presence of associated P- and R-branch transitions.

The same procedure could not be used for the $K_a = 1-0$ transitions. The lack of K -doubling in the $K_a = 0$ level of the lower electronic state meant that the transitions observed to levels with $K_a = 1$ in the upper state would show residual K -doubling and the magnitude of this K -doubling in the upper electronic state was unknown. Fortunately, the parameters determined from the $K_a = 0-1$ band were sufficient to allow $K_a = 1-0$ band to be assigned quite straightforwardly.

At this level of resolution second order effects tend to make certain misassignments obvious.

For example the off-diagonal element of the spin-tensor, $\frac{1}{2}|\epsilon_{ab} + \epsilon_{ba}|$, describes the interaction of levels differing in N and K by one unit. Thus when one spin component, $N = n$, in the $K = k$ stack has approximately the same energy as the same spin component with $N = n-1$, $K = k+1$ the two levels interact. The ensuing interaction is described by the off-diagonal element in the spin-tensor. This matrix element has only weak, if any, K dependence and thus tends to pin-point the crossing of the two K stacks. At the present resolution this is a very sensitive way to determine both the A rotational constant and the N numbering of the transitions. This particular perturbation can be seen in the residuals for one of the spin components. At $J = 17$ in the $v'_3 = 1 \rightarrow v''_3 = 0$ band the perturbation is a maximum with a positive residual. The residuals get progressively larger from lower J and suddenly become negative. This pattern was reproduced with residuals of the same magnitude in the corresponding P- and R- branches.

The fit was extended in an iterative procedure by predicting additional transitions and searching for appropriate matches. To a great extent the fits were limited to Q-branch

Comment [SHA15]: Minus sign changed to plus

1
2 transitions. This was because, within any one K -sub-band, the Q-branch transitions were
3 significantly more intense than the P- and R-branch transitions. Transitions which lie at
4 the high frequency end of the spectrum have also been, in some cases, difficult to assign.
5
6 This proved particularly so in the $K_a = 3-2$ sub-band of the $1_0^0 2_0^0 3_0^1$ vibrational band. The
7
8 most likely reason is that the energy levels are perturbed in some manner. This is not
9
10 surprising as the analogous band system in the HO_2 radical has been found [20] to be highly
11
12 perturbed. Given that the HS_2 radical has a higher density of states than HO_2 perturbations
13
14 are more likely. The relatively low signal to noise ratio and high line density of the present
15
16 spectra means that perturbations are neither easy to pick out nor to confirm by comparing
17
18 other transitions with common energy levels.
19
20

Comment [SHA16]: Numbering changed

21
22 The $1_0^0 2_0^0 3_0^1$ vibrational band was analysed first, simply because it was the strongest band in
23
24 which the transitions terminated in the vibrationless levels of all three vibrational modes. A
25
26 separate analysis was performed for the $1_0^0 2_0^0 3_0^0$ vibrational band. In both cases the microwave
27
28 and millimetre wave data from references 8 and 11 were included with weights appropriate to
29
30 the uncertainties of the measurements. The ground state parameters were allowed to float in
31
32 the analysis of the $1_0^0 2_0^0 3_0^0$ vibrational band but not in that of the $1_0^0 2_0^0 3_0^1$ vibrational band. This
33
34 allowed the ground state parameters to reflect the much larger values of N which were
35
36 assigned in the present work. A selection of the strongest Q-branch lines from the $\Delta K_a = +1$
37
38 and $\Delta K_a = -1$ sub-bands in each of the three bands analysed here are given in Table 3, along
39
40 with the residuals from the fit of each of the bands.
41
42

Comment [SHA17]: "shown" replaced by "given in Table 3"


Table 3 about here

43
44 Once reliable parameters for the $1_0^0 2_0^0 3_0^1$ vibrational band had been determined an analysis of
45
46 the $1_0^0 2_0^0 3_1^0$ band was undertaken. This proved to be relatively straightforward b
47
48 molecular parameters determined in the $v_3 = 1$ vibrational level are far less precise than those
49
50 in the $v_3 = 0$ level because the uncertainties of the Fourier transform data have higher
51
52
53
54
55
56
57
58
59
60

1
2 uncertainty than the microwave and millimetre wave data used to determine the parameters in
3
4 the $\nu_3 = 0$ level.

Table 4 about here

5
6 The K -sub-band structure in all the bands which have been observed is predominantly
7 perpendicular in nature ($\Delta K_a = \pm 1$). There is, however, evidence at low resolution [7] that
8 shows that significant parallel transition ($\Delta K_a = 0$) intensity must also be invoked in order to
9 model the band contour correctly. Parallel transitions have been sought in the high resolution
10 spectrum but no consistent results have been obtained. The line density is sufficiently high
11 that there are many coincidences between calculated and observed transitions but no branches
12 with $\Delta K_a = 0$ have been identified that can be traced with any certainty. Given that all the
13 necessary parameters for both the ground and excited states have been determined, the
14 parallel transitions should be straightforward to predict. It seems, therefore, that at the
15 present signal to noise ratio the parallel transitions are too weak to be picked out reliably,
16 even though sufficient intensity is present that, when integrated in a low resolution scan or
17 when a high resolution scan is convoluted, the overall band contour shows distinct parallel
18 character.

19
20 The usual expressions for the energy levels in asymmetric top molecules refer to five
21 centrifugal distortion parameters. This formulation has been shown to be over-determined in
22 the case of a planar molecule [25, 26] in which case only four are required. In the course of
23 the analysis the program was adapted to allow the fifth constant to be evaluated from the
24 other four. Although this did not allow us to determine more parameters than were varied, it
25 gave an important cross-check which ed useful when the higher-order terms were not
26 well determined.

Comment [SHA18]: Numbering
changed

Discussion

The data in Table 2 show that there is a very good agreement between the present low resolution data and the results of the high resolution analysis. The implication is that the maximum of the band at low resolution is in a consistent position with respect to the band origin. These are both consistent with earlier low resolution data [7]. It is obvious from Figure 1a that the bands involving excitation of ν_2 are much weaker and less well defined than the bands involving ν_3 and the uncertainty is correspondingly large.

One of the bands, shown in Figure 2 is assigned as having one quantum of vibration of ν_1 excited in the ground state. This is consistent with the calculated wavenumber of $2\,607\text{ cm}^{-1}$ from reference [18]. On the other hand an experimental wavenumber of $2\,463\text{ cm}^{-1}$ has been measured in a matrix [15] and the Franck-Condon factors reported in reference [4] show that the transitions involving ν_3 would be about one hundred times more intense than those involving ν_1 . This implies that transitions exciting ν_1 would not be observable in the current experiment. Although it could be argued that matrix effects have perturbed the frequency of the vibration there is no obvious reason for the far greater than expected intensity. It is, however, hard to envisage another assignment for the band assigned 1_1^0 here.

HS_2 has two heavy sulphur atoms which because of their mass lie very nearly on a principal inertial axis. This has the effect that although HS_2 is an asymmetric top it is very nearly at the limit of a prolate symmetric top. This can be shown by considering a measure such as Ray's asymmetry parameter κ , which is given by,

$$\kappa = \frac{(2B - A - C)}{(A - C)}$$

κ runs from -1 when the top is near prolate through zero in the very asymmetric case to $+1$ at the oblate limit. In this case for the lower state $\kappa = -0.99848$ and for the upper state $\kappa = -0.99868$ which are both almost indistinguishable from -1 . Hence the deviation from

Comment [SHA19]: Numbering changed.

Comment [SHA20]: Numbering changed.

(2) Comment [SHA21]: "1" replaced by "2"

Comment [SHA22]: Inserted

1
2
3
4
5
6
7
8
9
10
11
12
13
14
15
16
17
18
19
20
21
22
23
24
25
26
27
28
29
30
31
32
33
34
35
36
37
38
39
40
41
42
43
44
45
46
47
48
49
50
51
52
53
54
55
56
57
58
59
60

prolate symmetric top energy levels would be expected to be very small indeed. On the other hand the high density of states means that many unpredictable perturbations are possible.

Rotational constants have been determined for both $v_3=0$ and $v_3=1$ in both upper and lower states. This has allowed the determination of the vibrational dependence of the rotational constants on excitation of v_3 . The derived constants are given in Table 5. The derived parameters are denoted B_{00e} to indicate that the vibrational dependence of these parameters with respect to the v_1 and v_2 vibrations has not been taken into account. Table 5 about here

There have been many attempts to determine the structure of the HS₂ radical. Most of these have been through *ab initio* calculation [3, 16-18]. Saito *et al.* [8] have used the microwave spectra of HS₂ and DS₂ to try to determine both r_e and r_z structures. Of all previous structural calculations the rotational constants calculated in the most recent publication [18] are the closest to those determined here. In addition the structure of the radical in the \tilde{A}^2A' electronic state was calculated. The results for the excited state are qualitatively similar results to those calculated earlier by Sannigrahi *et al.* [4] but yield rotational constants which are closer to those observed. Obviously these parameters are not directly comparable as the *ab initio* calculation generates an equilibrium structure and in the present work only the vibrational dependence of the v_3 vibration has been taken into account.

The same study [18] also calculated the vibrational quanta in both \tilde{A}^2A' and \tilde{X}^2A'' states. These are given in Table 5 in comparison with the vibrational quanta determined here. It is interesting to note that the v_3 vibrational wavenumber decreases by nearly 20% whereas the rotational constants B_{00e} and C_{00e} decrease by only 10% and A_{00e} decreases by less than 3% on electronic excitation. This is consistent with the prediction [18] that the electronic excitation results primarily in the contraction of the bond angle and the lengthening of the SS

Comment [SHA23]: Numbering changed.

Comment [SHA24]: Numbering changed.

Comment [SHA25]: Numbering changed.

1
2 bond, the SH distance being essentially unchanged. It also accounts neatly for the fact that
3
4 the spectrum is primarily a progression in the ν_3 vibration.
5
6

7 **Acknowledgements**

8
9 We would like to thank the Alexander von Humboldt Stiftung which provided a travel grant
10 for SHA to work at Wuppertal University. SHA would also like to acknowledge the
11 encouragement and support received from Professor John M. Brown throughout his research
12 career and to thank him for the introduction to these data.
13
14
15
16
17
18
19
20
21
22
23
24
25
26
27
28
29
30
31
32
33
34
35
36
37
38
39
40
41
42
43
44
45
46
47
48
49
50
51
52
53
54
55
56
57
58
59
60

Comment [SHA26]: Text added

Figure Captions

Fig. 1. Overview spectra of the $\tilde{A}^2A' \rightarrow \tilde{X}^2A''$ transitions of HS_2 (a) and DS_2 (b) in the sensitivity range of the Ge detector. The resolution is 2 cm^{-1} .

Fig. 2. Section of the overview spectrum of HS_2 measured with the InSb detector at a resolution of 2 cm^{-1} . The asterisks mark strong atomic lines.

Fig. 3. Spectrum of the 000-000 and 001-001 bands of the $\tilde{A}^2A' \rightarrow \tilde{X}^2A''$ system of HS_2 at a nominal resolution of 0.01 cm^{-1} . The apodized line width is 0.016 cm^{-1} .

Fig. 4. Section of the high-resolution spectrum of the 001-000 band with rotational assignment of some Q-lines of the $K_a = 1-0$ sub-band.



Comment [SHA27]: "000-001" replaced by "001-000".

For Peer Review Only

Tables

Table 1

Wavenumbers of band maxima of the $\tilde{A}^2A' \rightarrow \tilde{X}^2A''$ transitions of HS_2 and DS_2 .

Band $00v_3' - 00v_3''$	HS_2 ν / cm^{-1}	DS_2 ν / cm^{-1}
0-0	7262.5(-1) ^a	7270.0(3)
0-1	6666.8(-1)	6674.9(-4)
0-2	6076.5(-1)	6087.6(-0)
0-3	5491.8(2)	
0-4	4912.0(-0)	
1-0	7766.9(2)	7772.2(-2)
1-1	7171.2(2)	7178.4(4)
1-2	6580.7(0)	
1-3	5995.5(-2)	
1-4	5416.3(2)	
1-5	4842.0(0)	
2-0	8266.2(-0)	8270.6(-2)
2-2	7080.0(-2)	
2-5	5341.3(-1)	
2-6	4772.8(2)	
3-0	8761.0(-0)	8765.2(1)
3-7	4703.9(-1)	
4-1	8655.5(1)	

^a Numbers in parentheses are the observed-calculated differences in units of the last digit.

Table 2.
Spectroscopic data of HS₂ and DS₂ obtained from the low-resolution analyses (in cm⁻¹).

		HS ₂		DS ₂		
		Experiment	Theory [7] ^a	Experiment	Theory [7]	
$\tilde{A}^2A' \rightarrow \tilde{X}^2A''$	000 – 000	7254(1) ^b 7254.035(5) ^c 7255(7) ^d	6936	7262(2) 7264(15) ^d	6936	
	000 – 001	6658(1) 6657.755(5) ^c		6667(2)		
	001 – 000	7758(1) 7758.693(5) ^c		7764(2)		
	001 – 010	6858(10)				
	000 – 010	6352(10)				
	010 – 020	6268(10)				
	000 – 100	4566(10)				
	\tilde{X}^2A''	ω_3^0	598.42(6)		597.7(9)	
		x_{33}^0	-2.692(9)		-3.33(48)	
		ν_3	595.73(7) 596.27996(44) ^c 595(4) ^d	559	594.4(10) 591(10) ^d	555
ν_2		892(10) 904(8) ^d 903 ^c	953	696(20) ^d	674	
ν_1		2688(10) 2463 ^c	2748		1966	
\tilde{A}^2A'		ω_3^0	506.46(9)		504.8(6)	
		x_{33}^0	-2.333(25)		-2.10(21)	
	ν_3	504.13(10) 504.533914(44) ^c 504(4) ^d	514	502.7(8) 502(15) ^d	511	
	ν_2	808(10)	838		593	
	ν_1		2775		1986	

Comment [SHA28]: Correction made to value

Comment [SHA29]: Correction made to value

^aMore theoretical data are found in Refs. [16-18] and [15].

^bNumbers in parentheses are estimated error limits or standard deviations of the parameters from fits in units of the last digit. Band origins of the low-resolution bands have been estimated by subtracting 8.5 cm⁻¹ from the wavenumbers of the characteristic peaks.

^cFrom high-resolution analyses.

^dResults of the low-resolution studies [7].

^eResults of an infrared absorption study in Ar matrices [15].

Comment [SHA30]: Numbering changed.

Comment [SHA31]: Numbering changed.

Comment [SHA32]: Numbering changed.

Table 3

Wavenumbers of selected lines of Q-branches observed in the $K = 1-0$ and $K = 0-1$ bands of the chemiluminescence spectrum of HS_2 . The deviations from the calculated values are included as an indication as the goodness of the fit.

N'	K'_a	K'_c	J'	N''	K''_a	K''_c	J''	$v'_3 = 0 \rightarrow v''_3 = 1$		$v'_3 = 0 \rightarrow v''_3 = 0$		$v'_3 = 1 \rightarrow v''_3 = 0$	
								Obs ^a	o-c ^b	Obs	o-c	Obs	o-c
1	0	1	1.5	1	1	1	1.5	6648.69514 *		7244.93959 *		7749.45549 *	
1	0	1	0.5	1	1	1	0.5	6647.28568 *		7243.58261 *		7748.09816 *	
2	0	2	2.5	2	1	2	2.5	6648.48291 *		7244.72342 *		7749.23356 *	
2	0	2	1.5	2	1	2	1.5	6647.36484 *		7243.65354 *		7748.16310 *	
3	0	3	3.5	3	1	3	3.5	6648.26163	2.14	7244.49236	-0.51	7748.99432 *	
3	0	3	2.5	3	1	3	2.5	6647.35163	1.46	7243.62648 *		7748.12714 *	
4	0	4	4.5	4	1	4	4.5	6648.01306	-1.15	7244.23485	-2.03	7748.72672 *	
4	0	4	3.5	4	1	4	3.5	6647.25791	1.75	7243.51674 *		7748.00556 *	
5	0	5	5.5	5	1	5	5.5	6647.74053	0.89	7243.94795 *		7748.42325 *	
5	0	5	4.5	5	1	5	4.5	6647.09379 *		7243.33559 *		7747.80966 *	
6	0	6	6.5	6	1	6	6.5	6647.43222	1.33	7243.62122 *		7748.07903 *	
6	0	6	5.5	6	1	6	5.5	6646.87180	1.37	7243.09054 *		7747.54691 *	
7	0	7	7.5	7	1	7	7.5	6647.08646	1.73	7243.25350 *		7747.69091 *	
7	0	7	6.5	7	1	7	6.5	6646.59187	0.92	7242.78637 *		7747.22213 *	
8	0	8	8.5	8	1	8	8.5	6646.69867	-0.34	7242.84271	0.00	7747.25720	0.45
8	0	8	7.5	8	1	8	7.5	6646.25847 *		7242.42621 *		7746.83841 *	
9	0	9	9.5	9	1	9	9.5	6646.27224 *		7242.38656	-0.82	7746.77798	2.83
9	0	9	8.5	9	1	9	8.5	6645.87319	-1.90	7242.01408	1.99	7746.39780 *	
10	0	10	10.5	10	1	10	10.5	6645.80201	-1.39	7241.88786	1.30	7746.24668	1.59
10	0	10	9.5	10	1	10	9.5	6645.44209	-0.15	7241.54596	0.58	7745.90166 *	
11	0	11	11.5	11	1	11	11.5	6645.29073	-0.99	7241.33994	0.45	7745.66470	-1.16
11	0	11	10.5	11	1	11	10.5	6644.96054	-0.34	7241.02702 *		7745.35093 *	
12	0	12	12.5	12	1	12	12.5	6644.73666 *		7240.74565 *		7745.03856	1.65
12	0	12	11.5	12	1	12	11.5	6644.43213	0.43	7240.45790	0.22	7744.74628 *	
13	0	13	13.5	13	1	13	13.5	6644.13718	-0.61	7240.10508	0.44	7744.35931	1.49
13	0	13	12.5	13	1	13	12.5	6643.85463	-0.57	7239.83782 *		7744.08818 *	
14	0	14	14.5	14	1	14	14.5	6643.49414	-0.63	7239.41546	-0.67	7743.62822	-0.09
14	0	14	13.5	14	1	14	13.5	6643.23199	0.26	7239.16827	0.48	7743.37696 *	
15	0	15	15.5	15	1	15	15.5	6642.80772	0.36	7238.67989 *		7742.84839	0.30
15	0	15	14.5	15	1	15	14.5	6642.56182	0.26	7238.44809	0.24	7742.61287 *	
16	0	16	16.5	16	1	16	16.5	6642.07562	0.30	7237.89549	-0.21	7742.01727	0.28
16	0	16	15.5	16	1	16	15.5	6641.84381	-1.08	7237.67889	0.72	7741.79610 *	
17	0	17	17.5	17	1	17	17.5	6641.29978	1.29	7237.06214	-1.25	7741.13404	-0.76
17	0	17	16.5	17	1	17	16.5	6641.08144	-0.41	7236.85859	-0.29	7740.92677 *	
18	0	18	18.5	18	1	18	18.5	6640.47753	0.82	7236.18263	-0.18	7740.20333	1.94
18	0	18	17.5	18	1	18	17.5	6640.27072	-1.81	7235.98878	-1.30	7740.00497 *	
19	0	19	19.5	19	1	19	19.5	6639.60913	-0.71	7235.25101	-2.83	7739.21756	0.95
19	0	19	18.5	19	1	19	18.5	6639.41669	-0.34	7235.07157	-0.26	7739.03078 *	
20	0	20	20.5	20	1	20	20.5	6638.69736	-0.40	7234.27612	-0.22	7738.18049	0.12
20	0	20	19.5	20	1	20	19.5	6638.51537 *		7234.10342	-0.76	7738.00424 *	
21	0	21	21.5	21	1	21	21.5	6637.74098	0.63	7233.25114	0.92	7737.09271	0.17
21	0	21	20.5	21	1	21	20.5	6637.56759 *		7233.08715 *		7736.92536 *	
22	0	22	22.5	22	1	22	22.5	6636.73739	-0.15	7232.17547	0.09	7735.95485	1.83
22	0	22	21.5	22	1	22	21.5	6636.57544	1.73	7232.02363	2.87	7735.79526	1.10
23	0	23	23.5	23	1	23	23.5	6635.68965	0.45	7231.05127	-0.46	7734.76156	-0.17

1														
2	23	0	23	22.5	23	1	23	22.5	6635.53504	1.31	7230.90622	1.22	7734.61164	1.00
3	24	0	24	24.5	24	1	24	24.5	6634.59529	0.04	7229.87917 *		7733.51970	1.13
4	24	0	24	23.5	24	1	24	23.5	6634.44925	1.62	7229.74104	1.18	7733.37569	0.90
5	25	0	25	25.5	25	1	25	25.5	6633.45620	0.60	7228.65792	0.29	7732.22299	-0.48
6	25	0	25	24.5	25	1	25	24.5	6633.31596	0.55	7228.52658	1.25	7732.08397	-2.64
7	26	0	26	26.5	26	1	26	26.5	6632.26992	-0.26	7227.38700 *		7730.87768	1.34
8	26	0	26	25.5	26	1	26	25.5	6632.13703 *		7227.26136 *		7730.74683	0.79
9	27	0	27	27.5	27	1	27	27.5	6631.03875	-0.13	7226.06648	-0.74	7729.47776	0.67
10	27	0	27	26.5	27	1	27	26.5	6630.91368	1.22	7225.94870	0.75	7729.35315	0.09
11	28	0	28	28.5	28	1	28	28.5	6629.76165 *		7224.69883	0.64	7728.02705	1.39
12	28	0	28	27.5	28	1	28	27.5	6629.64260	0.94	7224.58502 *		7727.90924	1.60
13	29	0	29	29.5	29	1	29	29.5	6628.43682	-1.56	7223.27950	-0.35	7726.52301	1.06
14	29	0	29	28.5	29	1	29	28.5	6628.32452	-0.07	7223.17345	0.89	7726.41219	2.44
15	30	0	30	30.5	30	1	30	30.5	6627.06894	-0.05	7221.81262	0.52	7724.96970	3.78
16	30	0	30	29.5	30	1	30	29.5	6626.96057	-0.65	7221.71050 *		7724.86114	1.80
17	31	0	31	31.5	31	1	31	31.5	6625.65181	-1.60	7220.29487 *		7723.35859	1.13
18	31	0	31	30.5	31	1	31	30.5	6625.55137	-0.10	7220.19879 *		7723.25890	2.54
19	32	0	32	32.5	32	1	32	32.5	6624.19165	0.10	7218.72716	-0.91	7721.69687	0.35
20	32	0	32	31.5	32	1	32	31.5	6624.09585	0.56	7218.63738 *		7721.60441	3.64
21	33	0	33	33.5	33	1	33	33.5	6622.68497	1.64	7217.11116	-0.46	7719.98440	1.39
22	33	0	33	32.5	33	1	33	32.5	6622.59337	0.73	7217.02621 *		7719.89248	-0.02
23	34	0	34	34.5	34	1	34	34.5	6621.12926	0.59	7215.44415	-1.27	7718.21910	2.23
24	34	0	34	33.5	34	1	34	33.5	6621.04597	2.53	7215.36521 *		7718.13480	3.29
25	35	0	35	35.5	35	1	35	35.5	6619.52711	-0.36	7213.72869	-0.72	7716.39791	-0.11
26	35	0	35	34.5	35	1	35	34.5	6619.44752	-0.11	7213.65452	0.20	7716.32103	3.28
27	36	0	36	36.5	36	1	36	36.5	6617.87934	-0.32	7211.96266	-0.84	7714.52915	2.76
28	36	0	36	35.5	36	1	36	35.5	6617.80527	0.14	7211.89406	0.62	7714.45424	3.08
29	37	0	37	37.5	37	1	37	37.5	6616.18515 *		7210.14759 *		7712.60258	0.67
30	37	0	37	36.5	37	1	37	36.5	6616.11615	0.25	7210.08395	1.40	7712.53385	2.17
31	38	0	38	38.5	38	1	38	38.5	6614.44195	-1.91	7208.22273	1.20	7710.62574	1.22
32	38	0	38	37.5	38	1	38	37.5	6614.38118	1.34	7208.28159 *		7710.56116	1.90
33	39	0	39	39.5	39	1	39	39.5	6612.65638	0.68	7206.36525	-0.18	7708.59285	-1.28
34	39	0	39	38.5	39	1	39	38.5	6612.59726	0.38	7206.31182	1.49	7708.53554	1.71
35	40	0	40	40.5	40	1	40	40.5	6610.82056	-0.01	7204.39901 *		7706.50695	-3.75
36	40	0	40	39.5	40	1	40	39.5	6610.76719	0.24	7204.35201	3.16	7706.45431	-1.03
37	41	0	41	41.5	41	1	41	41.5	6608.93770	-0.71	7202.38225 *		7704.37558	1.43
38	41	0	41	40.5	41	1	41	40.5	6608.88908	-0.89	7202.33675	-0.27	7704.32375 *	
39	42	0	42	42.5	42	1	42	42.5	6607.00910 *		7200.31504 *		7702.18409	-0.33
40	42	0	42	41.5	42	1	42	41.5	6606.96559	-0.28	7200.27476 *		7702.13795	-1.03
41	43	0	43	43.5	43	1	43	43.5	6605.03258 *		7198.19776	0.46	7699.94284	1.40
42	43	0	43	42.5	43	1	43	42.5	6604.99455 *		7198.16038	-1.60	7699.89683	-4.14
43	44	0	44	44.5	44	1	44	44.5	6603.00950	0.76	7196.02995	1.02	7697.64168	-3.48
44	44	0	44	43.5	44	1	44	43.5	6602.97631	0.37	7195.99860 *		7697.60663	-3.05
45	1	1	1	1.5	1	0	1	1.5	6668.51603 *		7264.79237 *		7769.34485 *	
46	1	1	1	0.5	1	0	1	0.5	6666.08331 *		7262.35961 *		7766.83166 *	
47	2	1	2	2.5	2	0	2	2.5	6666.69408 *		7262.96897 *		7767.43757 *	
48	2	1	2	1.5	2	0	2	1.5	6665.64722 *		7261.91694 *		7766.39049 *	
49	3	1	3	3.5	3	0	3	3.5	6666.60308 *		7262.86300 *		7767.33339 *	
50	3	1	3	2.5	3	0	3	2.5	6667.20432 *		7263.46417 *		7768.00285 *	
51	4	1	4	4.5	4	0	4	4.5	6666.44106 *		7262.68851	0.66	7767.15146	0.30
52	4	1	4	3.5	4	0	4	3.5	6666.93404 *		7263.18072 *		7767.70287 *	
53														
54														
55														
56														
57														
58														
59														
60														

1														
2	5	1	5	5.5	5	0	5	5.5	6666.21484 *	7262.44726	2.05	7766.89370	-4.02	
3	5	1	5	4.5	5	0	5	4.5	6666.63004 *	7262.86027 *		7767.36153	-2.23	
4	6	1	6	6.5	6	0	6	6.5	6665.92857 *	7262.13868	-0.54	7766.57684	-0.51	
5	6	1	6	5.5	6	0	6	5.5	6666.28582 *	7262.49734	1.03	7766.98008	1.06	
6	7	1	7	7.5	7	0	7	7.5	6665.58479 *	7261.77244 *		7766.19018	-2.58	
7	7	1	7	6.5	7	0	7	6.5	6665.89749 *	7262.08732	2.35	7766.54462 *		
8	8	1	8	8.5	8	0	8	8.5	6665.18724	2.10	7261.34651 *	7765.74056	-5.13	
9	8	1	8	7.5	8	0	8	7.5	6665.46282	0.14	7261.62319	-0.64	7766.05480	-3.23
10	9	1	9	9.5	9	0	9	9.5	6664.73217	1.45	7260.86251 *		7765.23493	-2.41
11	9	1	9	8.5	9	0	9	8.5	6664.97811	-1.73	7261.11135	-0.06	7765.51816	0.54
12	10	1	10	10.5	10	0	10	10.5	6664.22216	-0.11	7260.32120 *		7764.66534	-3.16
13	10	1	10	9.5	10	0	10	9.5	6664.44873	0.72	7260.54818	1.48	7764.92226	-0.07
14	11	1	11	11.5	11	0	11	11.5	6663.66023	-0.09	7259.72312 *		7764.03780	-1.98
15	11	1	11	10.5	11	0	11	10.5	6663.86769	1.15	7259.92905 *		7764.26576	-5.65
16	12	1	12	12.5	12	0	12	12.5	6663.04399	-1.30	7259.06907	0.42	7763.35070	-0.89
17	12	1	12	11.5	12	0	12	11.5	6663.23674	1.78	7259.25792	-0.10	7763.56426	-0.13
18	13	1	13	13.5	13	0	13	13.5	6662.37691	-0.55	7258.35862	0.51	7762.60471	0.42
19	13	1	13	12.5	13	0	13	12.5	6662.55565	2.68	7258.53403	0.74	7762.79758	-3.32
20	14	1	14	14.5	14	0	14	14.5	6661.65738	0.29	7257.59163	-0.10	7761.79623	-1.87
21	14	1	14	13.5	14	0	14	13.5	6661.82134	0.98	7257.75466 *		7761.98132	0.62
22	15	1	15	15.5	15	0	15	15.5	6660.88303	-1.33	7256.76962	-0.11	7760.93195	-1.31
23	15	1	15	14.5	15	0	15	14.5	6661.03847	1.48	7256.92358	1.60	7761.10295	-0.68
24	16	1	16	16.5	16	0	16	16.5	6660.05900	-0.45	7255.89224 *		7760.00950	-0.43
25	16	1	16	15.5	16	0	16	15.5	6660.20508	2.32	7256.03515 *		7760.17062	1.05
26	17	1	17	17.5	17	0	17	17.5	6659.18220	-0.30	7254.95889	-0.54	7759.03128	3.01
27	17	1	17	16.5	17	0	17	16.5	6659.31992	2.32	7255.09751	3.39	7759.18009	1.66
28	18	1	18	18.5	18	0	18	18.5	6658.25333	-0.30	7253.97333 *		7757.98777	-0.64
29	18	1	18	17.5	18	0	18	17.5	6658.38150 *		7254.09885 *		7758.13017 *	
30	19	1	19	19.5	19	0	19	19.5	6657.27315	0.19	7252.92780	-0.53	7756.88769	-2.78
31	19	1	19	18.5	19	0	19	18.5	6657.39443 *		7253.04933 *		7757.02477 *	
32	20	1	20	20.5	20	0	20	20.5	6656.24052	-0.09	7251.83036	0.08	7755.73426	-0.30
33	20	1	20	19.5	20	0	20	19.5	6656.35640 *		7251.94557 *		7755.86222 *	
34	21	1	21	21.5	21	0	21	21.5	6655.15703	0.35	7250.67579	-1.56	7754.51803	-2.76
35	21	1	21	20.5	21	0	21	20.5	6655.26512	-2.32	7250.78532	-2.27	7754.64253 *	
36	22	1	22	22.5	22	0	22	22.5	6654.02070	-0.57	7249.46907	-0.58	7753.24567	-3.58
37	22	1	22	21.5	22	0	22	21.5	6654.12590	-1.68	7249.57344	-1.99	7753.36161	-4.12
38	23	1	23	23.5	23	0	23	23.5	6652.83458	0.11	7248.20694	-0.35	7751.91813	-1.92
39	23	1	23	22.5	23	0	23	22.5	6652.93609	-0.76	7248.30676	-2.35	7752.02834	-3.51
40	24	1	24	24.5	24	0	24	24.5	6651.59592	-0.46	7246.89129	0.93	7750.53197	-1.31
41	24	1	24	23.5	24	0	24	23.5	6651.69446	-0.86	7246.98677	-1.93	7750.63611	-4.84
42	25	1	25	25.5	25	0	25	25.5	6650.30631	-0.80	7245.51858	-0.36	7749.08560	-3.44
43	25	1	25	24.5	25	0	25	24.5	6650.40254	-0.49	7245.61308	-1.18	7749.18846	-4.59
44	26	1	26	26.5	26	0	26	26.5	6648.96785	1.11	7244.09364	0.48	7747.58427	-3.16
45	26	1	26	25.5	26	0	26	25.5	6649.05912	-0.93	7244.18443	-1.41	7747.68639	-1.85
46	27	1	27	27.5	27	0	27	27.5	6647.57490	-0.47	7242.61375	0.66	7746.02796	-0.58
47	27	1	27	26.5	27	0	27	26.5	6647.66539	-1.05	7242.70351 *		7746.12371	-2.86
48	28	1	28	28.5	28	0	28	28.5	6646.13393	0.82	7241.07883 *		7744.41356	1.07
49	28	1	28	27.5	28	0	28	27.5	6646.22357	1.27	7241.16721	-0.14	7744.50793	-0.19
50	29	1	29	29.5	29	0	29	29.5	6644.63969	-0.34	7239.49065	0.16	7742.74087	1.52
51	29	1	29	28.5	29	0	29	28.5	6644.72768 *		7239.57690	-0.54	7742.83297 *	
52	30	1	30	30.5	30	0	30	30.5	6643.09533	-0.94	7237.84691	-1.25	7741.00980	0.56

1														
2	30	1	30	29.5	30	0	30	29.5	6643.18287	0.18	7237.93264	-1.22	7741.10172	0.51
3	31	1	31	31.5	31	0	31	31.5	6641.50202	0.11	7236.15145	-0.49	7739.22228 *	
4	31	1	31	30.5	31	0	31	30.5	6641.58772	0.32	7236.23572	-0.97	7739.30934	-3.57
5	32	1	32	32.5	32	0	32	32.5	6639.85673	-0.32	7234.40171	-0.24	7737.37673	-1.83
6	32	1	32	31.5	32	0	32	31.5	6639.94105	-0.86	7234.48544	-0.60	7737.46910	0.92
7	33	1	33	33.5	33	0	33	33.5	6638.16240	0.60	7232.59979	1.53	7735.47722	-0.98
8	33	1	33	32.5	33	0	33	32.5	6638.24693	0.63	7232.68186	-0.12	7735.56578	-1.35
9	34	1	34	34.5	34	0	34	34.5	6636.41598	-0.29	7230.74102 *		7733.51970	-1.61
10	34	1	34	33.5	34	0	34	33.5	6636.50162	0.93	7230.82394	-0.68	7733.60953	-0.30
11	35	1	35	35.5	35	0	35	35.5	6634.62056 *		7228.83034	0.04	7731.50760	-0.40
12	35	1	35	34.5	35	0	35	34.5	6634.70615	0.99	7228.91344	-0.62	7731.59499	-1.43
13	36	1	36	36.5	36	0	36	36.5	6632.77480 *		7226.86622 *		7729.43710	-1.31
14	36	1	36	35.5	36	0	36	35.5	6632.86020	0.37	7226.95128	0.89	7729.52665	-0.35
15	37	1	37	37.5	37	0	37	37.5	6630.87939	0.32	7224.84889 *		7727.31265 *	
16	37	1	37	36.5	37	0	37	36.5	6630.96457	-0.23	7224.93372 *		7727.40075	-0.94
17	38	1	38	38.5	38	0	38	38.5	6628.93204	-1.46	7222.77842 *		7725.13085 *	
18	38	1	38	37.5	38	0	38	37.5	6629.01881	-1.36	7222.86504	0.88	7725.21946	-1.14
19	39	1	39	39.5	39	0	39	39.5	6626.93821 *		7220.65491	-0.01	7722.89421	1.08
20	39	1	39	38.5	39	0	39	38.5	6627.02605 *		7220.74182 *		7722.98208	-1.80
21	40	1	40	40.5	40	0	40	40.5	6624.89331 *		7218.47766	-0.84	7720.60012	0.48
22	40	1	40	39.5	40	0	40	39.5	6624.98330	0.74	7218.56679 *		7720.68955	-2.08
23	41	1	41	41.5	41	0	41	41.5	6622.80073	1.83	7216.24867	-0.61	7718.25141	0.91
24	41	1	41	40.5	41	0	41	40.5	6622.88979 *		7216.33888	-0.32	7718.34513	1.13
25	42	1	42	42.5	42	0	42	42.5	6620.65503	-0.09	7213.96713	-0.23	7715.84651	0.65
26	42	1	42	41.5	42	0	42	41.5	6620.74788 *		7214.05914 *		7715.94110 *	
27	43	1	43	43.5	43	0	43	43.5	6618.46138	-0.69	7211.63088	-1.99	7713.38559	-0.27
28	43	1	43	42.5	43	0	43	42.5	6618.55694 *		7211.72726	0.52	7713.48611	3.01
29	44	1	44	44.5	44	0	44	44.5	6616.21987 *		7209.24592 *		7710.87063 *	
30	44	1	44	43.5	44	0	44	43.5	6616.31577	-1.29	7209.34209 *		7710.97012 *	

a The observed wavenumber of the lines in cm^{-1}

b The value of the $(\text{obs} - \text{calc}) \times 10^3$ in units of cm^{-1} . An asterisk indicates the line was given zero weight in the fit due to overlap or other perturbation and the quoted value is the calculated wavenumber.

Table 4

Molecular constants for the 000 and 001 levels of the \tilde{A}^2A' and \tilde{X}^2A'' states of HS_2 (in MHz) except where indicated.

Parameter	\tilde{A}^2A'		\tilde{X}^2A''	
	000	001	000	001
ν_0 / cm^{-1}	7254.035347(19) ^a	7758.569314(26)	0	6657.75539(44)
A	289615.1(74)	289500.8(37)	296978.9619(74)	296726.8(21)
B	7198.30(30)	7152.4363(56)	7996.36601(78)	7946.856(82)
C	7011.40(27)	6968.080(35)	7776.73845(80)	7727.770(71)
$\Delta_N \times 10^3$	6.182(82)	5.909(17)	5.88717(17)	5.875(22)
Δ_{NK}	0.2244(97)		0.2338296(85)	0.2272(26)
Δ_K	17.90(27)	18.36(29)	24.3299(11)	23.861(60)
$\delta_N^s \times 10^3$	0.20(10)	0.48(18)	0.155935(51)	0.172(27)
δ_K			0.13091(37)	
$\Phi_{NK} \times 10^6$			0.2479(74)	
$\Phi_{KN} \times 10^3$			0.03595(28)	
$\Phi_K \times 10^3$			8.32 ^b	
ϵ_{aa}	62440(72)	65120(429)	-45926.778(13)	-47556(18)
ϵ_{bb}	61.7(67)	67.7(12)	-424.287(13)	-420.2(18)
ϵ_{cc}	-271.5(61)	-265.41(92)	10.096(13)	8.8(14)
$\frac{1}{2} \epsilon_{ab} + \epsilon_{ba} $			235.416(74)	235.416 ^c
Δ_K^s	-450(31)	-452(29)	6.7205(22)	7.12(71)
$\Delta_{NK}^s + \Delta_{KN}^s$		-60(3)	-0.202128	0.15(13)
$\Delta_{NK}^s \times 10^3$			-9.528(66)	
$\Delta_N^s \times 10^3$			0.1787(33)	
δ_K^s			0.0976(67)	
$\delta_N^s \times 10^3$			6.18(23)	
Φ_K^s			-1.94(20)	

^a Numbers in parentheses are the standard deviations of the parameters in units of the last quoted decimal place.

^b Constrained at the value from [8].

^c Constrained at the value from the ground state.

Table 5
 Vibrational spacings and vibrational dependence of the rotational constants. All parameters in MHz except where indicated.

	$\tilde{A}^2 A'$	$\tilde{X}^2 A''$
$\Delta G(v_3 = 1-0) / \text{cm}^{-1}$	504.533914(44) ^a	596.27996(44)
$\Delta G(v_3 = 1-0) / \text{cm}^{-1}$ [18]	501	592
α_A	368.8(50)	252.1(21)
α_B	45.85(60)	49.505(83)
α_C	43.98(61)	48.969(72)
A_{00e}	289672.(32)	297105.0(11)
B_{00e}	7221.23(60)	8021.112(42)
C_{00e}	7033.39(58)	7801.223(37)

a Uncertainty given in units of last quoted decimal place.

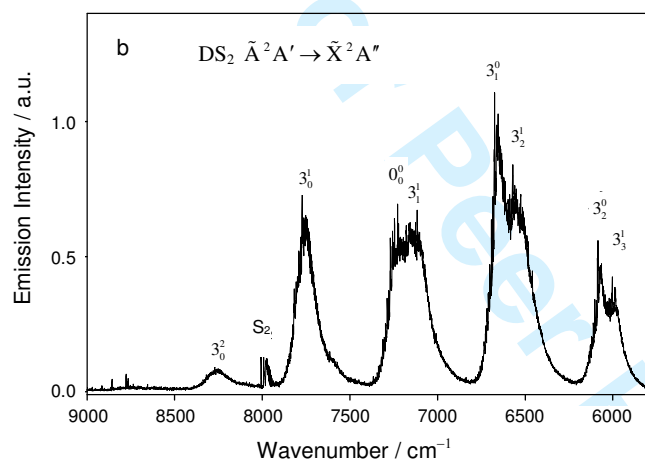
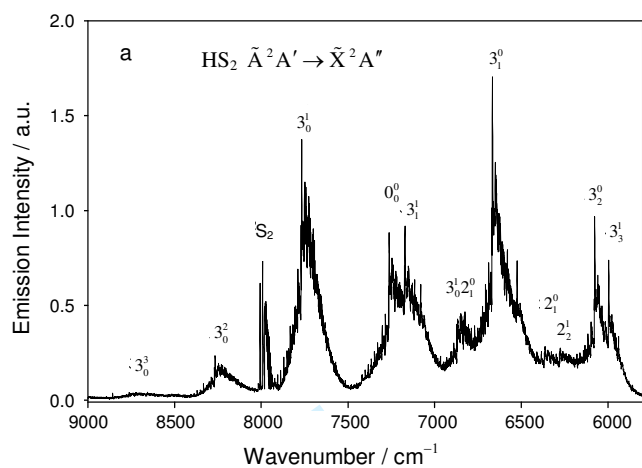


Figure 1

Figure 2

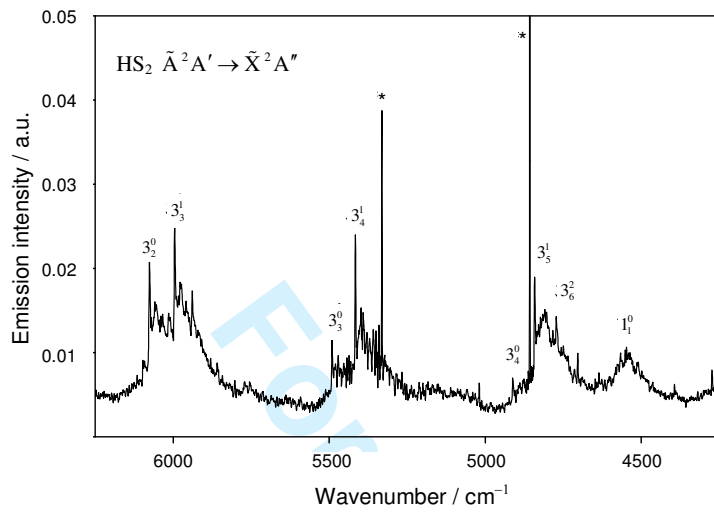


Figure 3

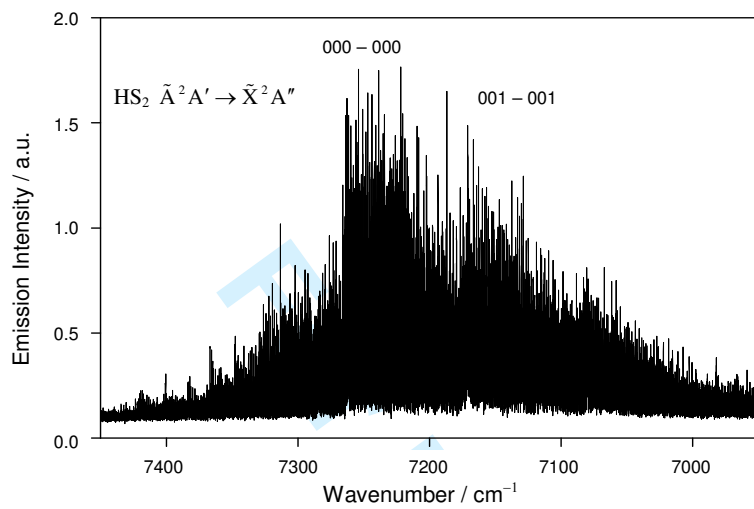
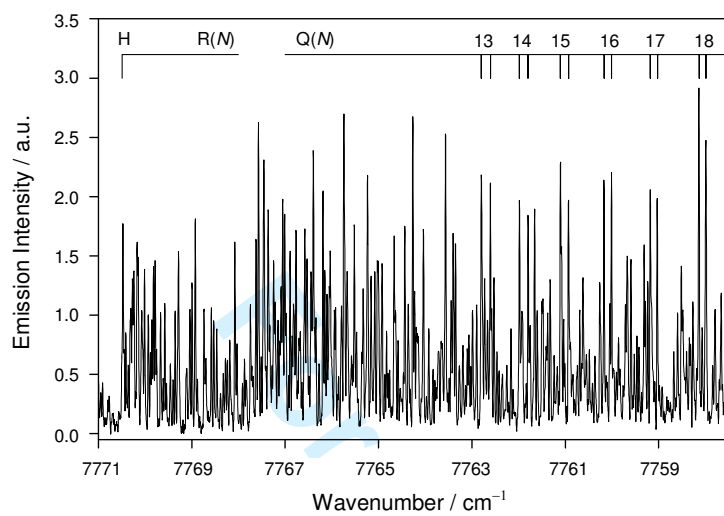


Figure 4



References

- 1 G. Porter, *Discussions of the Faraday Society*, 60-82 (1950)
- 2 O. P. Strausz, R. J. Donovan and M. De Sorigo, *Berichte der Bunsen-Gesellschaft*, **72**,
253-6 (1968)
- 3 R. K. Gosavi, M. Desorgo, H. E. Gunning and O. P. Strausz, *Chemical Physics
Letters*, **21**, 318-321 (1973)
- 4 A. B. Sannigrahi, S. D. Peyerimhoff and R. J. Buenker, *Chemical Physics Letters*, **46**,
415-421 (1977)
- 5 K. H. Becker, E. H. Fink, P. Langen and U. Schurath, *Journal of Chemical Physics*,
60, 4623-4625 (1974)
- 6 U. Schurath, M. Weber and K. H. Becker, *Journal of Chemical Physics*, **67**, 110-119
(1977)
- 7 K. J. Holstein, E. H. Fink, J. Wildt and F. Zabel, *Chemical Physics Letters*, **113**, 1-7
(1985)
- 8 S. Yamamoto and S. Saito, *Canadian Journal of Physics*, **72**, 954-962 (1994)
- 9 S. H. Ashworth and J. M. Brown, *Journal of Molecular Spectroscopy*, **153**, 41-58
(1992)
- 10 S. H. Ashworth, K. M. Evenson and J. M. Brown, *Journal of Molecular Spectroscopy*,
172, 282-295 (1995)
- 11 M. Tanimoto, T. Klaus, H. S. P. Muller and G. Winnewisser, *Journal of Molecular
Spectroscopy*, **199**, 73-80 (2000)
- 12 I. R. Slagle, R. E. Graham and D. Gutman, *International Journal of Chemical
Kinetics*, **8**, 451-458 (1976)
- 13 S. Glavas and S. Toby, *Journal of Physical Chemistry*, **79**, 779-782 (1975)
- 14 B. K. Decker, N. G. Adams and L. M. Babcock, *International Journal of Mass
Spectrometry*, **187**, 727-743 (1999)
- 15 E. Isoniemi, L. Khriachtchev, M. Pettersson and M. Räsänen, *Chemical Physics
Letters*, **311**, 47-54 (1999)
- 16 A. Hinchliffe, *Journal of Molecular Structure*, **66**, 235-242 (1980)
- 17 Q. Zhuo, D. J. Clouthier and J. D. Goddard, *Journal of Chemical Physics*, **100**, 2924-
2931 (1994)
- 18 P. A. Denis, *Chemical Physics Letters*, **422**, 434-438 (2006)
- 19 C. Aiot and J. Vergès, *Canadian Journal of Physics*, **59**, 1391-1398 (1981)
- 20 E. H. Fink and D. A. Ramsay, *Journal of Molecular Spectroscopy*, **185**, 304-324
(1992)
- 21 G. Osmann, P. R. Bunker, P. Jensen, R. J. Buenker, J. P. Gu and G. Hirsch, *Journal of
Molecular Spectroscopy*, **197**, 262-274 (1999)
- 22 G. Herzberg, *Molecular Spectra and Molecular Structure II. Infrared and Raman
Spectra of Polyatomic Molecules*, Krieger Publ. Co., Malabar, FL (1991) p.206
- 23 J. M. Brown and T. J. Sears, *Journal of Molecular Spectroscopy*, **75**, (1979)
- 24 T. J. Sears, *Computer Physics Communications*, **34**, 123-133 (1984)
- 25 J. M. Dowling, *Journal of Molecular Spectroscopy*, **6**, 550-553 (1961)
- 26 J. K. Watson, *Journal of Chemical Physics*, **46**, 1935-1949 (1967)

Comment [SHA33]: Numbering
changed

Comment [SHA34]: Numbering
changed

Comment [SHA35]: Numbering
changed

Comment [SHA36]: Numbering
changed

Comment [SHA37]: Citation added.

Comment [SHA38]: Numbering
changed

Comment [SHA39]: Citation added

Comment [SHA40]: Citation added.

Comment [SHA41]: Citation added.

Comment [SHA42]: Numbering
changed

Comment [SHA43]: Numbering
changed

Comment [SHA44]: Numbering
changed